



POLİTEKNİK DERGİSİ

JOURNAL of POLYTECHNIC

ISSN: 1302-0900 (PRINT), ISSN: 2147-9429 (ONLINE)

URL: <http://dergipark.org.tr/politeknik>



Investigation of structural, optical and electrical properties of Al_{0.3}Ga_{0.7}N/GaN HEMT grown by MOCVD

MOCVD ile büyütülen Al_{0.3}Ga_{0.7}N/ GaN HEMT'nin yapısal, optik ve elektriksel özelliklerinin araştırılması

Yazar(lar) (Author(s)): Ömer AKPINAR¹, Ahmet Kürşat BİLGİLİ², Mustafa Kemal ÖZTÜRK³, Süleyman ÖZÇELİK⁴, Ekmel ÖZBAY⁵

ORCID¹: 0000-0002-5172-8283

ORCID²: 0000-0003-3420-4936

ORCID³: 0000-0002-8508-5714

ORCID⁴: 0000-0002-3761-3711

ORCID⁵: 0000-0003-2953-1828

Bu makaleye şu şekilde atıfta bulunabilirsiniz (To cite to this article): Akpınar O., Bilgili A.K., Öztürk M.K., Özçelik S., and Özbay E., "Investigation of structural, optical and electrical properties of Al_{0.3}Ga_{0.7}N/GaN HEMT grown by MOCVD", *Politeknik Dergisi*, 23(3): 687-696, (2020).

Erişim linki (To link to this article): <http://dergipark.org.tr/politeknik/archive>

DOI: 10.2339/politeknik.583898

Investigation of Structural, Optical and Electrical Properties of $\text{Al}_{0.3}\text{Ga}_{0.7}\text{N}/\text{GaN}$ HEMT Grown by MOCVD

Highlights

- ❖ Comparison of the structural features of the structure grown with MOCVD with the literature
- ❖ Suitability of mobility and carrier density values of HEMT structure
- ❖ Optical results give similar results compared to previous studies

Graphical Abstract

In this study, the magnification phase of $\text{Al}_{0.3}\text{Ga}_{0.7}\text{N}/\text{GaN}$ HEMT structure and structural, optical and electrical properties after magnification were investigated.

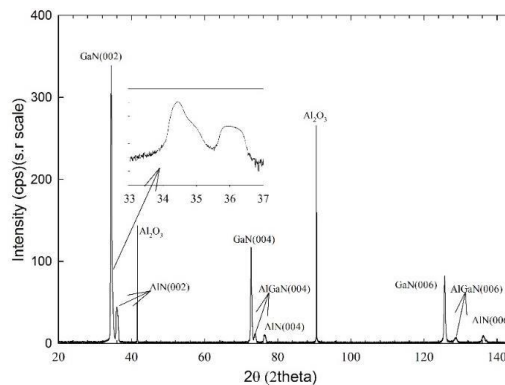


Figure A. 2θ -Intensity plot for $\text{Al}_{0.3}\text{Ga}_{0.7}\text{N}/\text{GaN}$ HEMT structure on symmetric planes

Aim

Comparison of the conformity of this structure with the literature, which was enlarged by the MOCVD method.

Design & Methodology

While building the structure, HEMT structure was created by MOCVD method.

Originality

It is a completely original work. These studies have not been done with the same material before.

Findings

The results I obtained after structural, optical and electrical measurements were observed to be compatible with the literature.

Conclusion

In this study AlGaIn/GaN HEMT structure is grown by MOCVD method. Optic, morphological and electric characterization of the samples are made with XRD, PL, UV-Vis, AFM and Hall-resistant measurements. 2θ , FWHM, lattice parameters, particle size, strain, stress and dislocation calculations are made on 19 different planes. Surface roughness of the sample is determined by morphological characterization. Hall-resistant measurements of the sample are made after taking the contacts by Van der Pauw method at 0.4 T constant magnetic field. In optical characterization according to PL measurement results 383 nm wavelength corresponds to 3.24 eV. This value is in fact the direct band gap of GaN. In UV-Vis the conduction of AlGaIn layer started at 360 nm that corresponds to 3.48 eV. In morphological characterization low RMS showed that the sample has good surface quality. It is noticed that carrier density is not effected by the temperature and mobility is high. It is assumed that the slight increase on carrier density at high temperature is caused by the annealing effect. On the other hand, as the temperature decrease mobility increase.

Declaration of Ethical Standards

The authors of this article declare that the materials and methods used in this study do not require ethical committee permission and/or legal-special permission.

MOCVD ile Büyütülen Al_{0.3}Ga_{0.7}N/GaN HEMT'nin Yapısal, Optik ve Elektriksel Özelliklerinin Araştırılması

Araştırma Makalesi / Research Article

Ömer AKPINAR^{1,2*}, A. Kürşat BİLGİLİ¹, M. Kemal ÖZTÜRK^{1,2}, Süleyman ÖZÇELİK^{1,2}, Ekmel ÖZBAY³

¹Department of Physics, Gazi University, 06500 Ankara, Turkey

²Photonics Research Center, Gazi University, 06500 Ankara, Turkey

³Nanotechnology Research Center, Bilkent University, 06800 Ankara, Turkey

(Geliş/Received : 28.06.2019 ; Kabul/Accepted : 18.07.2019)

ÖZ

Bu çalışmada c-eksenli safir alttaş üzerine MOCVD yöntemiyle büyütülen Al_{0.3}Ga_{0.7}N/GaN yüksek elektron hareketli transistör (HEMT) yapısı incelenmiştir. Bu yapının optik, morfolojik ve elektriksel özellikleri X-Işını Kırınımı (XRD), Fotoluminesans (PL), Ultraviyole ve görünür ışık (UV-Vis), Atomik Kuvvet Mikroskobu (AFM) ve Hall-Direnç ölçümleri ile belirlendi. Simetrik ve asimetrik düzlemlerde XRD metodu ile 2θ, Yarım Maximum'daki Tam Genişlik (FWHM), örgü parametreleri, kristal boyutu, zorlama, gerilme ve dislokasyon değerleri hesaplanmıştır. GaN'nin doğrudan bant aralığı PL ölçümleriyle 3.24 eV olarak belirlenir. AlGa_{0.3}N katmanının iletiminin UV-Vis'de 360 nm'de başladığı görülmektedir. Hall-Direnç ölçümlerinde, HEMT yapısının taşıyıcı yoğunluğunun sıcaklıktan etkilenmediği ve hareketlilik değerinin yüksek olduğu ölçüldü. Taşıyıcı yoğunluğu ve hareketlilik değerleri oda sıcaklığında sırasıyla 5.82x10¹⁵ 1/cm³ ve 1198 cm²/V olarak belirlendi. En düşük sıcaklık değerinde (25 K) sırasıyla 5.19x10¹⁵ 1/cm³ ve 6579 cm²/V olarak hesaplandı.

Anahtar Kelimeler: HEMT, XRD, zorlama, gerilme, hall.

Investigation of Structural, Optical and Electrical Properties of Al_{0.3}Ga_{0.7}N/GaN HEMT Grown by MOCVD

ABSTRACT

In this study, Al_{0.3}Ga_{0.7}N/GaN high electron mobility transistor (HEMT) structure is investigated grown over c- oriented sapphire substrate by using Metal Organic Chemical Vapor Deposition (MOCVD) method. Structural, optical, morphological and electrical characteristics of this structure are determined by X-ray diffraction (XRD), Photoluminescence (PL), Ultraviolet (UV-Vis.), Atomic Force Microscopy (AFM) and Hall- Resistivity measurements. By using XRD method, 2θ, Full Width at Half Maximum (FWHM), lattice parameters, crystallite size, strain, stress and dislocation values are calculated on symmetric and asymmetric planes. Direct band gap of GaN is determined by PL measurements as 3.24 eV. It is seen that conduction of AlGa_{0.3}N layer starts at 360 nm in UV-Vis. In Hall-Resistivity measurements, it is noticed that carrier density of HEMT structure is not effected by temperature and mobility value is high. Carrier density and mobility values are determined as 5.82x10¹⁵ 1/cm³ and 1198 cm²/V.s at room temperature, respectively. At the lowest temperature point (25 K) they are calculated as 5.19x10¹⁵ 1/cm³ and 6579 cm²/Vs, respectively.

Keywords: HEMT, XRD, strain, stress, hall.

1. INTRODUCTION

HEMT is a field effect transistor in which different band ranges and polarization fields are enlarged as two layers. HEMTs are used in many areas due to their ability to work at high frequencies and high temperatures. It is used in radar systems, automotive applications, sensors, computer systems etc. [1-3]

There are many fields that conventional III-V group semiconductors are not used. Short wave length light emitters are needed for colour screens, laser writers, and high density data storage and under water

communication. Transistors resistant to high power and high temperature are needed for some fields such as automobile motors, developed power distribution systems and many other electric devices. Si and conventional III-V group semiconductors are not suitable for desinging and producing optoelectric devices on blue and ultraviolet region of the spectrum. Gallium Arsenide (GaAs) based electric devices are not used at high temperatures. Group III nitrides are suitable for applications in this field. Group III nitrides has wide and direct band gap. Band gap values are 0.7, 3.4 and 6.2 eV for Indium nitride (InN), Gallium nitride (GaN), and Aluminium nitride (AlN) respectively [4, 5]. Properties such as wide band gap and strong chemical bonds makes

* Sorumlu yazar (Corresponding Author)
e-posta : omerakpinar9@gmail.com

them convenient for blue, green and ultraviolet light emitting devices and transistors resistant to high temperature [6].

Towards the end of 20th century, Shuji Nakamura made it easier to grow high quality GaN epitaxial layer over sapphire (Al₂O₃) substrate by using MOCVD method [7]. GaN based structures gave way to new developments in optoelectronics. At the same time GaN with its high electron mobility has excellent electron carrying properties and forming large electric field capability [8]. If the properties above are combined, GaN based HEMT has better properties than GaAs. Its power density can be increased to a determined level.

AlGaIn/GaN structure presents many advantages for high power and high frequency communication according to Si and other III-V group compound semiconductors [9]. Discontinuation of high conduction band, causes large layer charge density at AlGaIn/GaN interface for %35 Al compound bigger than $1 \times 10^{13} \text{ cm}^{-2}$ [10]. Large band gap of GaN and AlGaIn maintains big defect fields and thermal stability of the material permishes to operate at high temperature. These perfect properties caused forming devices which has 1.5 A/mm high current density [11], 1 kV deterioration potential difference [12], 11.2 W/mm power density at 10 GHz [13]. Other than optoelectronic applications, this HEMT structure has an important role in nitride hetero structures, emitter stations for satellite communications etc. [14].

2. EXPERIMENTAL

In this study, electrical, optical, structural and surface morphological properties of AlGaIn/GaN heterostructure semiconductor sample, grown over c-oriented sapphire substrate by MOCVD method, are investigated.



Figure.1 Schematic Diagram of AlGaIn/GaN HEMT structure grown over Sapphire substrate

Before growth of the mentioned structure, sapphire substrate is annealed at 1100 °C for 10 minutes under hydrogen flow [15]. After 60 seconds nitridation step, temperature is decreased to 550 °C. AlN and HT-AlN layers are grown between substrate and GaN buffer layer. To perform this step first temperature and reactor pressure are increased to 750 °C and 50 mbar respectively. Later, under 300sccm NH₃ flow, nitridation operation is performed. By adding 15 sccm TMAI flow LT-AlN nucleation layer is grown for 3 minutes. This layer is a preparation layer for the next HT-AlN layer and this layer is responsible for the low dislocation density at HT-AlN layer. After growth of LT-AlN nucleation layer, temperature is increased to 1130 °C in 4 minutes. This quick increase in temperature maintained annealing of LT-AlN structure having a amorphous structure. At the end of this operation it is aimed LT-AlN layer to shift to a mono-crystal structure. After annealing operation, for growth of 520 nm thick HT-AlN layer under 25 mbar pressure, 25 sccm TMAI and 150 sccm NH₃ flow is decreased to 40sccm in 60 seconds. This flow rate is kept constant for growth of remaining HT-AlN layer. Because mobility of Al atoms on the surface of the substrate is low, high growth temperature is needed for high crystal quality. On the other hand, during growth of HT-AlN 50 sccm Trimetilindium (TMIn) flow is maintained. Presence of In atoms increases the mobility of Al atoms but In atoms can not diffuse in AlN at this temperature [16]. HT-AlN layer has a duty as a barrier against O atoms in Al₂O₃ substrate. O atoms changes the electric properties of GaN by passing through it so that GaN has lower resistivity. HT-AlN layer prevents difusing of O atoms into GaN layer so it helps forming a high resistivity (HR) GaN buffer layer. After growth of HT-AlN layer 90 nm thick first GaN layer is grown under 200 mbar pressure and 1300 sccm NH₃, 10 sccm TMGa flow at 1000 °C. Later in five minutes temperature and NH₃ flow are increased to 1050 °C and 1500 sccm, respectively. Under these circumstances second GaN layer is grown with a thickness of 800 nm. By increasing the temperature to 1060 °C, NH₃ and TMGa flow rates to 1800 and 17 sccm respectively, third GaN layer with a thickness of 110 nm is grown. After this step only temperature is increased to 1075 °C and 300 nm thick GaN layer is grown. Later, at 1050 °C and 750 °C temperatures GaN layers with thicknesses of 150 nm and 5 nm are grown respectively. Reactor parameters are changed for growth of 1-2 nm thick AlN layer. Reactor pressure and NH₃ flow is decreased to 50 mbar and 210 sccm respectively. Temperature is kept constant and 10 sccm TMAI flow is given. For growth of 25 nm AlGaIn barrier layer, 5 sccm TMGa and 500 sccm NH₃ flow is given. Finally, TMAI flow is stopped and all other parameters are kept constant for growth of 3 nm thick GaN cap layer.

3. RESULT AND DISCUSSION

Electrical, optical, structural and surface morphological properties of $\text{Al}_{0.3}\text{Ga}_{0.7}\text{N}/\text{GaN}$ HEMT sample grown by MOCVD method is investigated.

3.1. XRD

2θ versus intensity plot is shown in Figure 2. On (002) plane GaN, AlGa N and AlN are not fully distorted from each other but it can be seen that on (004) and (006) planes they are distorted from each other. The small figure in figure 2 is the detailed image belonging to (002) plane. Diffraction peaks of GaN layer for (002), (004) and (006) planes are 34.789, 73.018 and 126.016 respectively. Diffraction peaks of AlGa N layer are 35.202, 74.195 and 129.088 and for AlN layer they are 36.221, 76.494 and 136.448 respectively. As understood from peak positions GaN is in accordance with AlGa N and AlN and all structures are compatible with hexagonal crystal system.

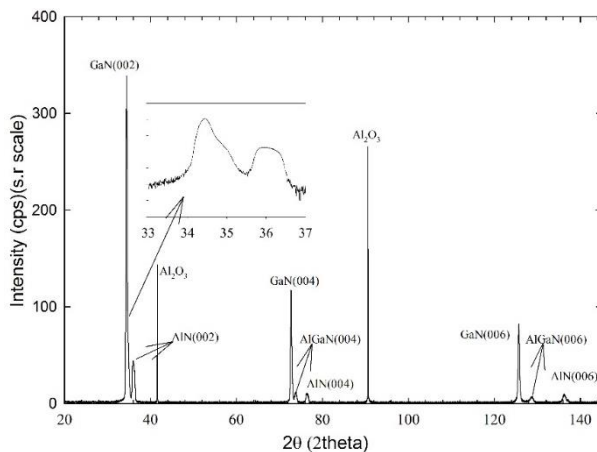


Figure 2. 2θ -Intensity plot for $\text{Al}_{0.3}\text{Ga}_{0.7}\text{N}/\text{GaN}$ HEMT structure on symmetric planes

In Figure 3. 2θ -Intensity plot is given on asymmetric (011), (012), (013) and (014) planes. Here in (hkl) orientation hk is kept constant and planes on “ T ” direction are chosen. In some layers peak broadening is caused from AlGa N layer so AlGa N structure can be seen clearly as FWHM on GaN decrease and “ T ” increase. AlGa N structure is in hexagonal shape crystallographilly and it is compatible with Vegard law and Al alloy ratio shows triclinic structure behaviour. On (011) and (012) planes AlN is in the position that it can not be distorted from GaN and AlGa N . As “ T ” increases before AlGa N is distorted, peak width of AlN increases to a higher value. But on (014) plane as AlGa N is fully distorted from GaN, AlN peak width decrease. Crystal quality can be understood in more detail by the analysis of FWHM values for these layers. In figure 3, XRD plot for (021), (022), (023) and (024) planes is given. As “ T ” values are changed by keeping hk values constant it is seen that on (021) plane structure is not fully distorted but when the plane values increase structure is fully distorted. It is noticed that peak widths of GaN and AlN layers decrease by distortion of the structure. These results are valid for

peak positions in Figure 4 also. By changing the plane values structure can be examined in detail.

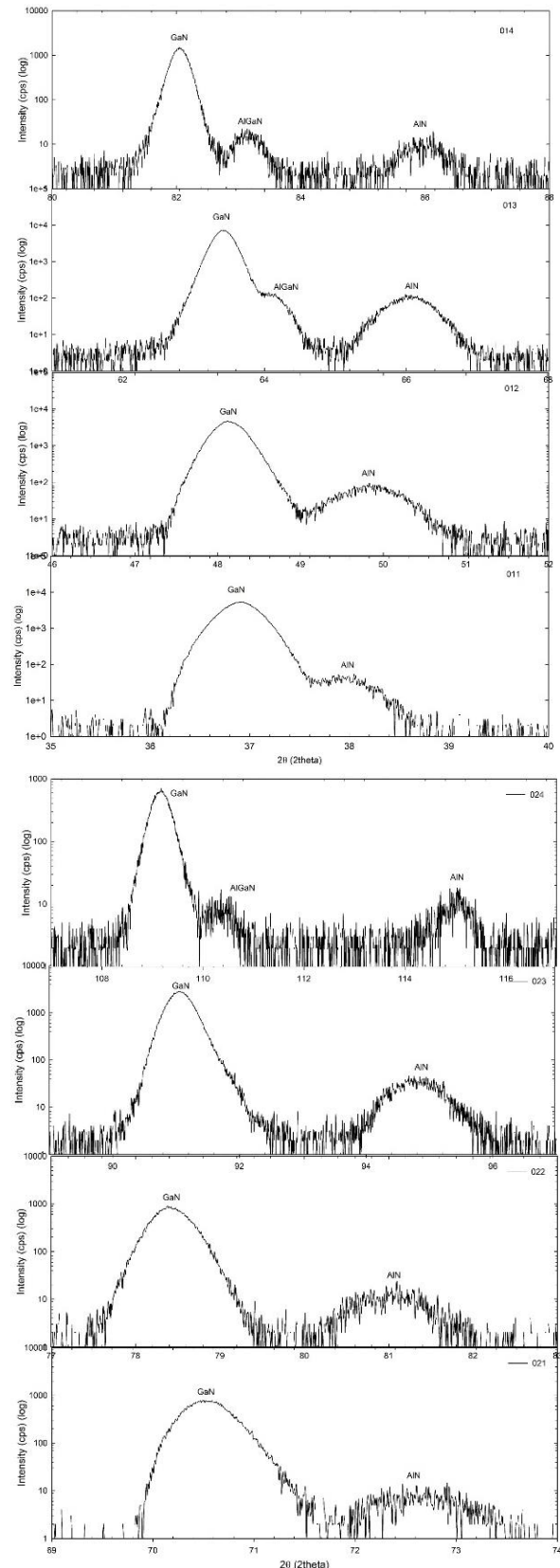


Figure 3. XRD plots for $\text{Al}_{0.3}\text{Ga}_{0.7}\text{N}/\text{GaN}$ HEMT structure on asymmetric (011), (012), (013), (014), (021), (022), (023) and (024) planes

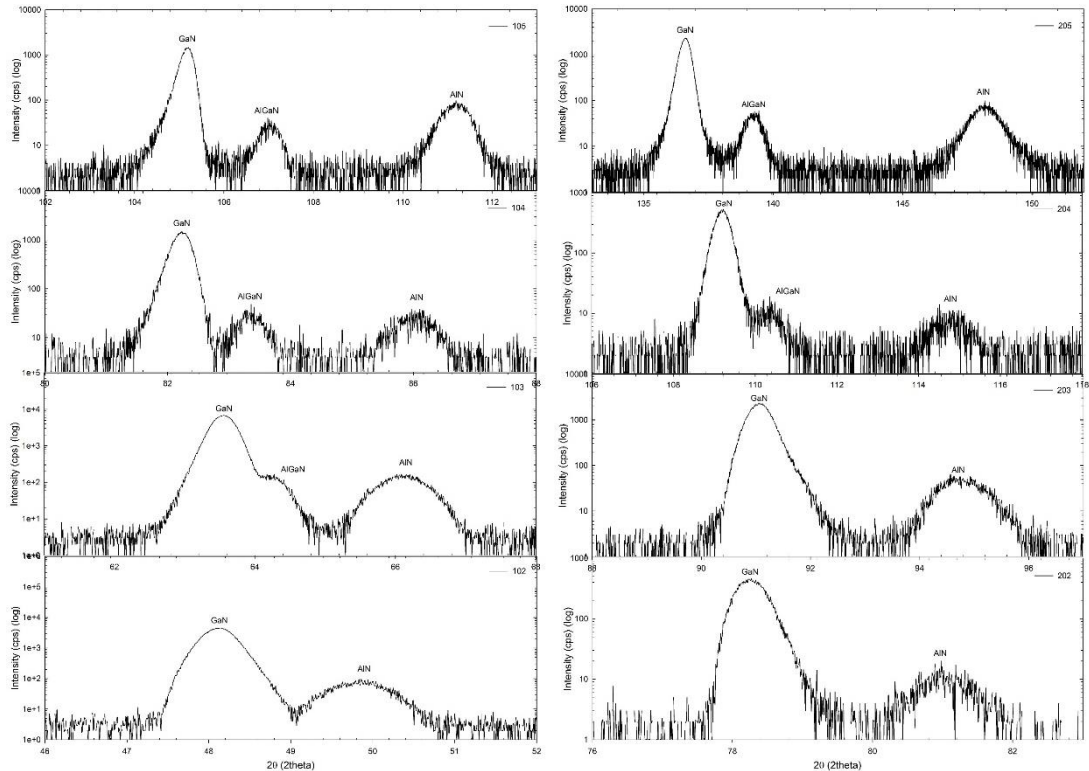


Figure 4. XRD plots for $Al_{0.3}Ga_{0.7}N/GaN$ HEMT structure on (102), (103), (104), (105), (202), (203), (204) and (205) asymmetric planes

Table.1 2θ and FWHM values on (hkl) planes for GaN, AlGaIn and AlN layers

Plane (hkl)	GaN		AlGaIn		AlN	
	2θ	FWHM(deg)	2θ	FWHM(deg)	2θ	FWHM(deg)
002	34.739	0.250	35.202	0.338	36.221	0.744
004	73.018	0.248	74.195	0.414	76.494	0.462
006	126.016	0.258	129.088	0.166	136.448	0.320
011	36.905	0.422	-	-	38.058	0.248
012	48.127	0.390	-	-	49.831	0.303
013	63.418	0.321	64.056	0.453	65.995	0.507
014	82.051	0.288	83.112	0.386	86.076	0.159
021	70.526	0.524	-	-	72.608	0.063
022	78.400	0.445	-	-	81.094	0.064
023	91.054	0.429	-	-	94.755	0.037
024	109.178	0.420	110.356	0.035	115.045	0.043
202	78.250	0.507	-	-	80.983	0.078
203	91.068	0.471	-	-	94.793	0.067
204	109.200	0.436	110.395	0.214	114.758	0.092
205	136.619	0.450	139.453	0.229	148.228	0.088
102	48.123	0.434	-	-	49.864	0.304
103	63.550	0.377	64.183	0.078	66.076	0.088
104	82.236	0.361	83.256	0.125	86.040	0.112
105	105.187	0.326	107.017	0.051	111.195	0.502

FWHM is related with crystal quality of epitaxial layers. 2θ and FWHM values on symmetric and asymmetric (hkl) planes for GaN, AlGa_N and AlN layers are given in Table 1. When the angle increase on (002), (004) and (006) planes, variation on FWHM values determines crystal quality. On asymmetric planes when the angle values increase FWHM values decrease. The reason for this is the peak width. Low FWHM value means high crystal quality, low dislocation density and more smooth structure.

diffraction angles on symmetric and asymmetric planes for GaN, AlGa_N and AlN layers. As the angle value increase, particle size also increases

Tilt, lateral and vertical length values for GaN, AlGa_N and AlN values are given in Table 3. Tilt values for GaN, AlGa_N and AlN layers are 4.2x10⁻³, 1.4x10⁻³ and 1.9x10⁻³ nm, respectively. For the same layers lateral length values are 539.26, 33.27 and 19.29 nm and vertical lengths are 3.08x10⁻⁴, 5.59x10⁻⁴ and 11.2x10⁻⁴ nm, respectively. As can be seen, as lateral length increase,

Table 2. Lattice parameters a-, c-, and particle size (D) values for GaN, AlGa_N and AlN layers

Plane (hkl)	GaN			AlGa _N			AlN		
	a(nm)	c(nm)	D(nm)	a(nm)	c(nm)	D(nm)	a(nm)	c(nm)	D(nm)
002	-	5.158	34.68	-	5.092	25.76	-	4.954	11.73
004	-	5.176	41.52	-	5.106	25.11	-	4.975	22.85
006	-	5.184	70.75	-	5.116	116.24	-	4.975	69.95
011	3.182	5.174	20.72	-	-	-	3.089	5.023	35.30
012	3.185	5.180	23.29	-	-	-	3.083	5.013	30.16
013	3.188	5.184	30.41	3.160	5.138	21.62	3.077	5.003	19.50
014	3.187	5.183	38.11	3.154	5.129	28.72	3.066	4.985	71.10
021	3.187	5.182	19.40	-	-	-	3.108	5.053	161.25
022	3.187	5.183	24.04	-	-	-	3.099	5.039	169.16
023	3.189	5.186	27.62	-	-	-	3.093	5.029	323.55
024	3.187	5.183	34.06	3.164	5.146	409.63	3.079	5.007	353.87
102	3.186	5.180	20.95	-	-	-	3.081	5.010	30.03
103	3.182	5.174	25.91	3.154	5.129	124.24	3.074	4.998	111.92
104	3.182	5.173	30.47	3.150	5.121	88.80	3.067	4.987	101.41
105	3.184	5.177	41.92	3.146	5.115	273.78	3.065	4.984	29.24
202	3.192	5.191	21.10	-	-	-	3.102	5.044	139.45
203	3.189	5.185	25.13	-	-	-	3.092	5.027	181.73
204	3.187	5.182	32.86	3.164	5.144	67.95	3.084	5.015	167.25
205	3.186	5.181	49.87	3.156	5.132	104.24	3.078	5.006	341.63

Lattice parameter values in Table 2 are very similar with theoretical values [17]. Particle size changes with

vertical length decrease for GaN, AlGa_N and AlN structures.

Table 3. Tilt, lateral and vertical length values for GaN, AlGa_N and AlN layers

	Tilt(°)(x10 ⁻³)	Lateral L.(nm)	Vertical L.(nm)(x10 ⁻⁴)
GaN	4.2	539.26	3.08
AlGa _N	1.4	33.27	5.59
AlN	1.9	19.29	11.2

Table 4. Dislocation values for GaN, AlGaN and AlN layers

	Edge Dis. (cm ⁻²)(x10 ⁹)	Screw Dis.(cm ⁻²)(x10 ⁹)
GaN	5.26	1.98
AlGaN	1.40	0.52
AlN	3.02	1.14

Edge and screw type dislocation values are given in Table 4. Edge dislocation values for GaN, AlGaN and AlN layers are 5.26x10⁹, 1.40x10⁹ and 3.02x10⁹ cm⁻², respectively and screw type dislocation values are 1.98x10⁹, 0.52x10⁹ and 1.14x10⁹ cm⁻², respectively.

Edge dislocation value is the highest in GaN layer but the least in AlGaN layer. The same situation is present for screw type dislocation values. The values given in Table 4 are the average values.

value for GaN shows just the opposite behaviour according to AlGaN and AlN. That is the stress is on negative direction. Stress values for AlN are higher than GaN and AlGaN. The reason for this is the difference between covalent radiusus of Ga, N and Ga, Al and N for GaN and AlGaN layers respectively. Inverse stresses that are seen in all structures shows differences in different structures. In addition to these if symmetric and asymmetric planes are examined carefully, as 2θ value

Table 5. Strain and stress values for GaN, AlGaN and AlN layers on (hkl) planes

Plane (hkl)	GaN		AlGaN		AlN	
	Strain (x10 ⁻⁴)	Stress (GPa)(x10 ⁻³)	Strain (x10 ⁻⁴)	Stress (GPa) (x10 ⁻³)	Strain (x10 ⁻⁴)	Stress (GPa) (x10 ⁻³)
002	1.86	-33.01	-5	27.93	-7.7	-197.72
004	1.32	-66.02	-3.6	-6.99	-4	158.11
006	0.04	69.32	-7.6	31.45	-10.9	356.09
011	-30.6	-281.1	-	-	-1761.8	-870.48
012	-2.3	-533.26	-	-	-3.9	-1397.3
013	-285.3	-525.7	-1	-246.28	-0.95	-1113.32
014	-2.1	-364.55	-5.3	-384.95	-5.2	-609.42
021	-1.8	-577.1	-	-	5.3	-1434.54
022	-6.6	-702.51	-	-	2.7	-663.25
023	-5.7	-714.2	-	-	1.2	-2537.85
024	-4.4	-543.45	-12.3	-1049.75	-12.7	-860.65
102	-3.2	-588.29	-	-	-16	-1559.25
103	-2.1	-525.51	-3.3	-36.93	-0.1	-1322.42
104	-2.5	-364.63	-2.4	-154.05	5	-1392.39
105	-3.5	-176.27	-3.2	-27.95	-12.8	-2004.02
202	-8.8	-842.85	-	-	-23	-2405.42
203	-8.4	-873.32	-	-	-12.6	-1975.86
204	-6.6	-543.74	-28	-954.6	1.3	-1506.5
205	-2	-309.57	79.9	7302.65	-6.8	-359.02

In Table 5, strain and stress values for three symmetric and sixteen asymmetric planes of GaN, AlGaN and AlN. Stress values determines interplanar pressing. Stress

increase stress values also increase. If strain values are examined, it can be seen that all three layers show different behaviour. As stress values increase strain

values also increase in GPa degree. This may be as a result of interplanar inhomogeneity.

In Figure 5, lateral and vertical WH plots are given. The plot drawn by using $\sin\theta$ gives lateral WH and the plot drawn by using $\cos\theta$ gives vertical WH. In Figure 5, WH plots for GaN, AlGaN and AlN layers are shown. The disorders in the structures are described by $y=ax+y_0$ linear equation. Here Y axis intercept of this plot gives lateral and vertical block length y_0 . The equations gained from lateral and vertical WH plots for GaN are $y=45.8x-5.6$ and $y=-35.9x-349.2$ respectively. R^2 values are 0.99

and 0.96 respectively. R^2 values nearer to 1 means that the structure is more crystallised. The equations gained from lateral and vertical WH plots for AlGaN are $y=13.9x+135.2$ and $y=72.8x+559$ respectively. R^2 values for this layer are 0.10 and 0.72 respectively. This result means that crystal quality is not good. Equations gained from lateral and vertical WH plots for AlN are $y=18.5x+233.3$ and $y=-166.4x+1118.9$ respectively. R^2 values for this layer are 0.86 and 0.99 respectively. High crystal quality of these layers are supported by the FWHM values in the previous section of this article.

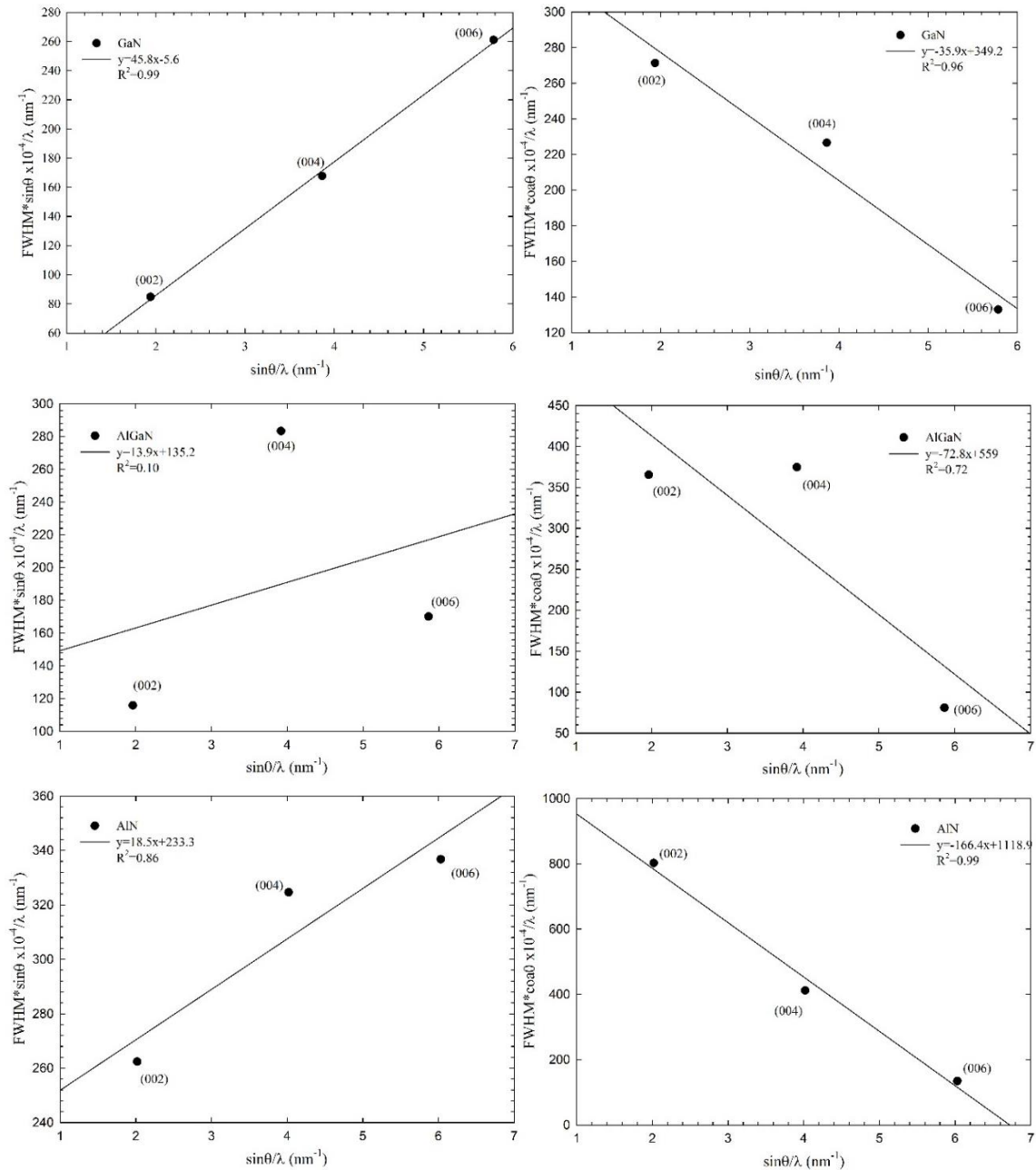


Figure 5. Lateral (on the left) and vertical (on the right) WH plots of GaN, AlGaN and AlN layers on symmetric and asymmetric planes

3.2. Resistance and Hall Effect measurements

In this study, 8 resistance and 8 Hall measurements are performed. Resistance measurement can be performed by using Van der Pauw geometry. Van der Pauw samples can be prepared without lithography. Van der Pauw resistance equation is given in equation (1) [18].

$$e^{-\frac{\pi d}{\rho} R_{12,34}} + e^{-\frac{\pi d}{\rho} R_{23,41}} = 1 \tag{1}$$

$R_{12,34}$ is the current applied through contacts. Potential difference between the contacts is $V_4 - V_3$ and it is given in equation (2) [19].

$$R_{12,34} = \frac{V_4 - V_3}{I_{12}} = \frac{V_{34}}{I_{12}} \tag{2}$$

In order to simplify the solution of resistance Van der Pauw writes the equation (1) again as a function of thickness (d). The equation gained by this operation is given in equation (3) [19].

$$\rho = \frac{\pi d}{\ln 2} \left(\frac{R_{12,34} + R_{23,41}}{2} \right) f \left(\frac{R_{12,34}}{R_{23,41}} \right) \tag{3}$$

Here f is described as the correction factor of Van der Pauw and is given by equation (4) [19].

$$\frac{R_{12,34} - R_{23,41}}{R_{12,34} + R_{23,41}} = \frac{f}{\ln 2} \operatorname{arccosh} \left(e^{\frac{\ln 2 / f}{2}} \right) \tag{4}$$

In order to minimize the effect of extra potentials 8 different measurements are made.

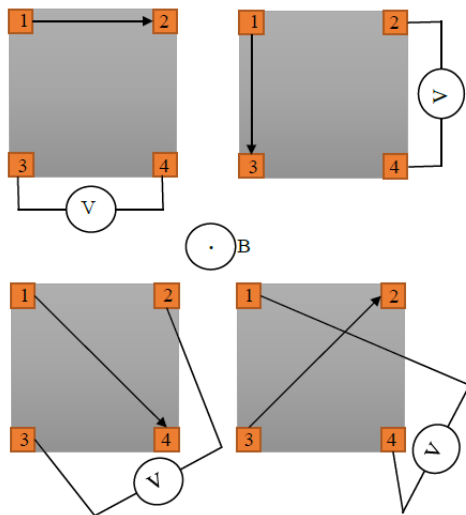


Figure 6. Schematic diagram of 4 different resistance measurement on Van der Pauw sample

In Figure 6 arrows shows the direction of current. Hall Effect voltage (V_H) is given by equation (5).

$$V_H = Ew = \frac{BI}{ent} \tag{5}$$

In this equation B is the magnetic field, w is the width of the sample and e is the charge of the charge carrier. Hall coefficient R_H is given by equation (6).

$$R_H = \frac{V_H t}{BI} \tag{6}$$

Hall mobility of the carriers μ_H and carrier density n are given by equations (7) and (8) respectively.

$$\mu_H = \frac{R_H}{\rho} \tag{7}$$

$$n_H = \frac{1}{eR_H} \tag{8}$$

Resistance measurements of $Al_{0.3}Ga_{0.7}N/GaN$ structure is made at 25-330 K range by using Van der Pauw method. During these measurements magnetic field is kept constant at 0.4 T resistance versus temperature plot without magnetic field is given in Figure 7. $Al_{0.3}Ga_{0.7}N/GaN$ HEMT structure shows metallic behaviour in temperature dependent measurements and at lower temperatures it shows resistance.

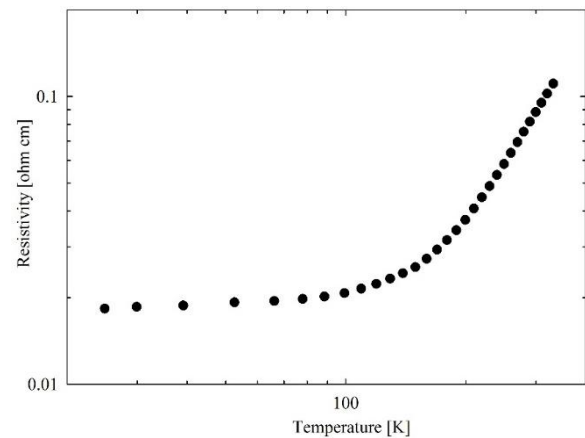


Figure 7. Variation of resistance dependent on temperature for $Al_{0.3}Ga_{0.7}N/GaN$ HEMT structure

The sample presented negative behaviour that shows R_H free carriers are electrons. Temperature dependent both carrier density and mobility of the considered sample are shown in Figure 8.

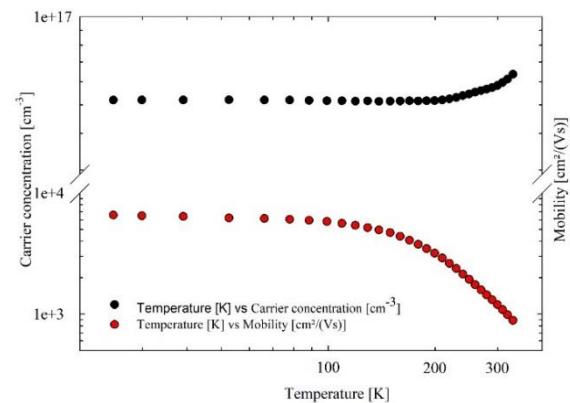


Figure 8. Temperature dependent both carrier density and mobility of the considered sample

As can be seen in Figure 8 if temperature is lower than 100 K mobility is independent on temperature. If temperature is higher than 100 K it shows a decreasing behaviour. This result is caused by the optic phonon diffraction. At higher temperatures optic phonon diffraction is dominant. Carrier density is almost independent of temperature at 25-330 K range. At higher temperatures carriers may cause a little increase because of annealing. The slight increase in the carrier density dependent on temperature may be caused by the oxygen defects in GaN layers. Mobility and carrier density are measured as 1198 cm²/Vs and 5.82x10¹⁵ 1/cm³ at room temperature respectively. At 25 K mobility and carrier density are measured as 6579 cm²/Vs and 5.19x10¹⁵ 1/cm³ respectively.

3.3. Photoluminescence (PL)

Photoluminescence (PL) is one of the most common optical characterisation technique for III-V group semiconductors because of its simple and strong measuring property. PL is used for determining quality of and performance of the devices and their defect states [20].

The energy values gained from PL peaks can be used in determining energy gaps and analysing defect density of the materials. At the same time material quality can be calculated by the FWHM and peak density. As can be seen in Figure 9 peak position is at 383 nm (3.24 eV) and FWHM is 4.27 nm.

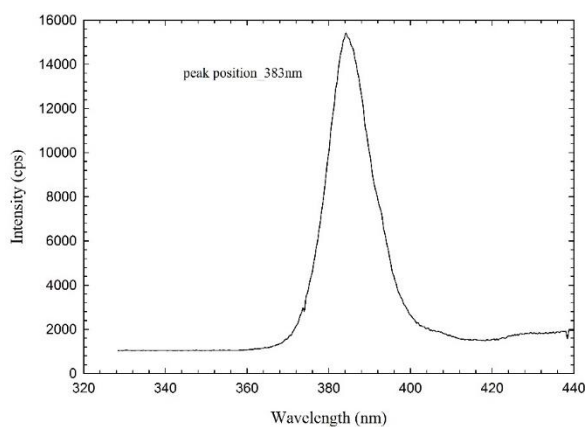


Figure 9. PL spectra of GaN layer

3.4. UV-Vis Spectrometer

Band gap and refraction index of the semiconductors can be determined from absorption and transmission spectras. Transmission can be transformed to optical absorption coefficient of the material by using equation (9). Taking into account of the sample absorption coefficient as a function of the energy can be gained. Equation (10) shows the relation between absorption coefficient and band gap.

$$a = \log\left(\frac{1}{T}\right) \quad (9)$$

$$ahv = A\sqrt{hv - E_g} \quad (10)$$

Here A is a constant and hv is the energy of the incident photon. Optical conduction measurement results are given in Figure 10. Conduction starts at 360 nm which corresponds to approximate value of 3.48 eV.

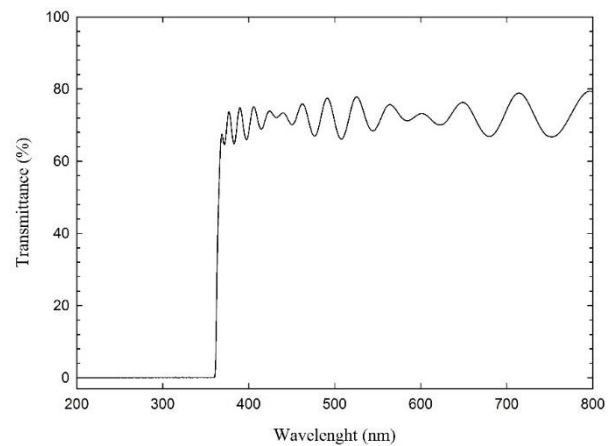


Figure 10. Optical conduction measurement for AlGaIn layer

3.5. Force Microscopy (AFM)

AFM scanning results in 5x5μm² scanning area are given in Figure 11. As can be seen the structure is in step-terrace structure. The terraces in the image are caused by the mixed and screw type dislocations. The structure has 1.61 nm Root Mean Square (RMS) value. This RMS value shows that surface quality is good.

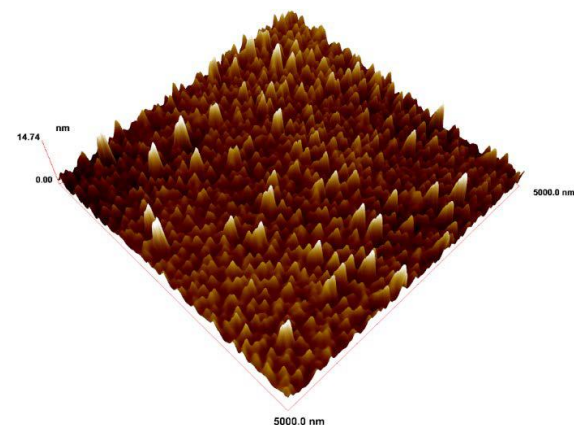


Figure 11. AFM Scanning image

4. CONCLUSION

In this study AlGaIn/GaN HEMT structure is grown by MOCVD method. The sample is prepared in 5mm x 5mm size. Optic, morphological and electric characterisation of the samples are made with XRD, PL, UV-Vis, AFM and Hall-resistant measurements. 2θ, FWHM, lattice parameters, particle size, strain, stress and dislocation calculations are made on 19 different planes. Material quality and conduction properties of the sample are determined by optical characterisation. Surface roughness of the sample is determined by morphological

characterisation. Hall- resistant measurements of the sample are made after taking the contacts by Van der Pauw method at 0.4 T constant magnetic field. In optical characterisation according to PL measurement results 383 nm wavelength corresponds to 3.24 eV. This value is in fact the direct band gap of GaN. This measurement showed the high crystal quality of GaN by high peak density and narrow FWHM. In UV-Vis the conduction of AlGaIn layer started at 360 nm that corresponds to 3.48 eV. In morphological characterisation low RMS showed that the sample has good surface quality. It is noticed that carrier density is not effected by the temperature and mobility is high. It is assumed that the slight increase on carrier density at high temperature is caused by the annealing effect. On the other hand, as the temperature decrease mobility increase.

ACKNOWLEDGEMENTS

This work was supported by the Presidency Strategy and Budget Directorate (Grants Numbers: 2016K121220).

REFERENCES

1. Yildirim R., Yavuzcan H.G., Celebi F.V. and Gokrem L., "Temperature dependent Rolletti stability analysis of GaN HEMT", *Optoelectronics and Advanced Materials-Rapid Communications*, 3(8): 781-786, (2009).
2. Gokrem L., Celebi F.V. and R. Yildirim, "Asymmetric amplitude variation for four tone small signal input gan hemt at different temperatures", *Journal of the Faculty of Engineering and Architecture of Gazi University*, 25(4): 779-786, (2010).
3. Yu H.B., Lisesivdin S.B., Bolukbas B., Kelekci O., Ozturk M.K., Ozcelik S., Caliskan D., Ozturk M., Cakmak H., Demirel P. and Ozbay E., "Improvement of breakdown characteristics in AlGaIn/GaN/AlxGa1-xN HEMT based on a grading AlxGa1-xN buffer layer", *Physica Status Solidi a-Applications and Materials Science*, 207(11): 2593-2596, (2010).
4. Akpinar O., Bilgili A.K., Ozturk M.K., Ozcelik S. and Ozbay E., "On the elastic properties of INGAN/GAN LED structures", *Applied Physics a-Materials Science & Processing*, 125(2): (2019).
5. Vurgaftman I. and Meyer J.R., "Band parameters for nitrogen-containing semiconductors", *Journal of Applied Physics*, 94(6): 3675-3696, (2003).
6. Ponce F.A. and Bour D.P., "Nitride-based semiconductors for blue and green light-emitting devices", *Nature*, 386(6623): 351-359, (1997).
7. Nakamura S., Gan Growth Using Gan Buffer Layer, *Japanese Journal of Applied Physics Part 2-Letters*, 30(10a): L1705-L1707, (1997).
8. Xing H., Keller S., Wu Y.F., McCathy L., Smorckova I.P., Buttari D., Coffie R., Green D.S., Parish G., Heikman S., Shen L., Zhang N., Xu J.J., Keller B.P., DeBaaars S.P and Mishra U.K., Gallium nitride based transistors, *Journal of Physics-Condensed Matter*, 13(32): 7139-7157, (2001).
9. Ghione G., Chen K.J., Egawa T., Meneghesso G., PalaciosT. and Quay R., Special Issue on GaN Electronic Devices, *Ieee Transactions on Electron Devices*, 60(10): 2975-2981, (2013).
10. Ambacher O., Foutz B., Smart J., Shealy J.R., Weimann N.G., Chu K., Murphy M., Sierakowski A.J., Schaff W.J., Eastman L.F., Dimitrov R., Mitchell A. and Stutzmann M., Two dimensional electron gases induced by spontaneous and piezoelectric polarization in undoped and doped AlGaIn/GaN heterostructures. *Journal of Applied Physics*, 87(1): 334-344, (2000).
11. Moon J.S., Micovic M., Janke P., Hashimoto P., Wong W.S., Widman R.D., McCray L., Kurdoghlian and Nguyen C., GaN/AlGaIn HEMTs operating at 20GHz with continuous-wave power density > 6W/mm, *Electronics Letters*, 37(8): 528-530, (2001).
12. Zhang N.Q., Moran B., DenBaars S.P., Mishra U.K., Wang X.W. and Ma T.P., Kilovolt AlGaIn/GaN HEMTs as switching devices, *Physica Status Solidi a-Applied Research*, 188(1): 213-217, (2001).
13. Shealy J.R., Kaper V., Tilak V., Prunty T., Smart J.A., Green B. and Eastman L.F., An AlGaIn/GaN high-electron-mobility transistor with an AlN sub-buffer layer, *Journal of Physics-Condensed Matter*, 14(13): 3499-3509, (2002).
14. Eastman L.F., Tilak V., Kaper V., Smart J., Thompson R., Green B., Shealy J.R. and Prunty T., Progress in high-power, high frequency AlGaIn/GaN HEMTs, *Physica Status Solidi a-Applied Research*, 194(2): 433-438, (2002).
15. Porowski S., Grzegory I., Kolesnikov D., Lojkowski W., Jager V., Jager W., Bogdano V., Suski T. and Krukowski S., Annealing of GaN under high pressure of nitrogen, *Journal of Physics-Condensed Matter*, 14(44): 11097-11110, (2002).
16. Zhang L.B., Yan H., Zhu G., Liu S. and Gan Z.Y., Molecular dynamics simulation of aluminum nitride deposition: temperature and N : Al ratio effects, *Royal Society Open Science*, 5(8), (2018).
17. Dridi Z., Bouhafs B. and Ruterana P., First-principles investigation of lattice constants and bowing parameters in wurtzite AlxGa1-xN, InxGa1-xN and InxA11-xN alloys, *Semiconductor Science and Technology*, 18(9): 850-856, (2003).
18. Tokarska M., Evaluation of Measurement Uncertainty of Fabric Surface Resistance Implied by the Van der Pauw Equation, *IEEE Transactions on Instrumentation and Measurement*, 63(6): 1593-1599, (2014).
19. Van der Pauw L.J., A method of measuring specific resistivity and Hall effect of discs of arbitrary shape, *Philips Technical Review*, 13(1): 1-9, (1958).
20. Swaminathan V. and MacRander A.T., Materials Aspects of Gaas and Inp Based Structures (Prentice Hall Advanced Reference Series): Prentice Hall, (1991).